

Phonons and structures of tetracene polymorphs at low temperature and high pressure

Elisabetta Venuti, Raffaele Guido Della Valle, Luca Farina, and Aldo Brillante
*Dipartimento di Chimica Fisica e Inorganica and INSTM-UdR Bologna,
 Università di Bologna, Viale Risorgimento 4, I-40136 Bologna, Italy*

Matteo Masino and Alberto Girlando
*Dipartimento di Chimica G.I.A.F. and INSTM-UdR Parma,
 Università di Parma, Parco Area delle Scienze, I-43100, Parma, Italy*
 (Dated: May 8, 2021)

Crystals of tetracene have been studied by means of lattice phonon Raman spectroscopy as a function of temperature and pressure. Two different phases (polymorphs I and II) have been obtained, depending on sample preparation and history. Polymorph I is the most frequently grown phase, stable at ambient conditions. Application of pressure above 1 GPa yields polymorph II, which is also obtained by cooling the sample below 140 K. However, the conditions for inducing the phase transitions depend on sample preparation and history, and polymorph II can also be maintained at ambient conditions. We have calculated the crystallographic structures and phonon frequencies as a function of temperature, starting from the configurations of the energy minima found by exploring the potential energy surface of crystalline tetracene. The spectra calculated for the first and second deepest minima match satisfactorily those measured for polymorphs I and II, respectively. The temperature dependence of the spectra is described correctly. All published x-ray structures, once assigned to the appropriate polymorph, are also reproduced.

PACS numbers: 63.20.-e, 81.30.Hd, 78.30.-j

I. INTRODUCTION

Among molecular organic semiconductors, oligoacenes crystals represent a subject of increasing experimental and theoretical interest, because their high carrier transport properties make them likely candidates for applications in electronic and opto-electronic devices.^{1,2,3} New techniques have been exploited for the growth of acene ultrapure single crystals^{2,3,4} or thin solid films,⁵ with the aim of obtaining high quality, well ordered crystalline samples. In fact, the absence of structural defects is crucial for the achievement of optimal performances in charge carrier mobilities.³

Much effort has been devoted to clarify the polymorphism of pentacene.^{6,7,8,9,10} Starting from all the published x-ray structures for crystalline pentacene,^{10,11,12,13} we computed the structures of minimum potential energy, and obtained two local minima of the potential energy, i.e., two different “inherent structures” of mechanical equilibrium.⁶ This behavior indicated that there were at least two different single crystal polymorphs of pentacene. The calculations predicted significant differences between the corresponding Raman spectra of the lattice phonons, which we checked experimentally, confirming the existence of two polymorphs.⁷ The correct identity of the samples, initially assigned only by matching experimental and calculated spectra, was thus verified directly with x-ray diffraction measurements. Finally, we obtained theoretical information on the global stability of the minima by systematically sampling the potential surface of crystalline pentacene.⁸ We found that the two polymorphs correspond to the two deepest minima. Fur-

ther deep minima with layered structures, which might correspond to the thin film polymorphs found to grow on substrates, were also predicted.

The existence of high temperature (HT),^{12,13} low temperature (LT) and high pressure (HP) polymorphs^{14,15,16,17,18,19,20,21} of tetracene has been known and studied in the past, and has been reported recently in studies on electronic transport in tetracene single crystals.^{3,22} Phase transitions for this system seem indeed to occur under variable conditions, depending on sample preparation, history and cooling speed.^{3,18,19,22} As the transformations are sluggish, the sample can show a large temperature range in which more than one structure is present, and important hysteresis effects can be observed. Generally, this results in lowered carrier mobilities and shattering of the crystal upon cooling. Altogether, however, not much is known about the characteristics of the transitions and the nature of the polymorphs involved. For instance, it is not clear yet how many phases are actually formed at low temperature, or whether a LT phase does correspond to the HP one.

In this paper we address the issue of polymorphism in tetracene with the methods already successfully used for pentacene polymorphs. First, we provide lattice phonon Raman spectra obtained by means of a microprobe technique for two different phases of solid tetracene as a function of both temperature and pressure. Interfacing optical microscopy to Raman spectroscopy allows for a detailed mapping of the physical features of each crystalline sample and probe the conditions under which more phases can be simultaneously present. Secondly, ex-

perimental data are compared with the results of quasi harmonic lattice dynamics^{23,24,25} (QHLD) calculations performed by using either the available crystallographic data,^{12,13,19} or the theoretical predictions of the most stable crystal structures for this system, which were obtained by performing a systematic sampling of the potential energy surface,²⁶ as already done for pentacene.

II. EXPERIMENTAL

High temperature crystalline tetracene (HT structure) can be obtained by sublimation under vacuum of the commercial product (Aldrich) as thin platelets of the length of a few mm and thickness of tenths of μm . Samples of microcrystalline powder obtained by a fast sublimation process may instead contain domains of the low temperature (LT) structure as physical impurity. Sublimation in an inert atmosphere at reduced pressures (10–20 kPa of nitrogen or argon) at 493 K, with a procedure similar to that used to obtain polymorph II of pentacene,⁷ yielded directly larger amount of physically pure LT phase.

Raman scattering has been detected by using several laser lines, eventually selecting low energy excitation from a krypton laser tuned at 752.5 nm to minimize sample fluorescence, due perhaps to some residual chemical impurities.³ Raman spectra above 1 GPa were anyway overlapped by strong fluorescence in all conditions. The spectra have been collected and analysed by the Jobin Yvon T64000 spectrometer equipped with a liquid nitrogen cooled CCD detector. Low temperatures T down to 80 K were achieved in a conventional cryostat (Linkam HFS 91) with a temperature gradient of 10 K/min. High pressures p up to 6 GPa were obtained in a LOTO diamond anvil cell,²⁷ using perfluorocarbon as pressure medium. Pressures were measured with the ruby luminescence method.²⁸

Low T and high p cells were placed on the stage of the microscope (Olympus BX40) directly interfaced to the spectrometer. The use of 20x and 50x magnification objectives allowed for a spatial resolution of 2.2 and 1.1 μm , respectively, yielding the possibility to spatially check the physical purity of crystal polymorphs by mapping the lattice phonon profiles along the sample surface.⁷

III. COMPUTATIONAL METHODS

The crystal structures and vibrational frequencies of tetracene have been calculated with the same procedure used for pentacene,^{7,8,29} following a well assessed treatment.^{30,31} We first compute *ab-initio* molecular geometry, atomic charges, vibrational frequencies and cartesian eigenvectors of the normal modes for the isolated tetracene molecule. This is done with the Gaussian98 program³² (Rev. A.5), using the 6-31G(d) basis set combined with the B3LYP exchange correlation

functional.^{32,33} The vibrational frequencies are scaled by the factor of 0.9613 recommended^{34,35} for the combination of B3LYP and 6-31G(d).

The crystal total potential energy Φ is given in terms of an atom-atom Buckingham model,³⁶ with Williams parameter set IV,³⁷ combined with an electrostatic contribution represented by a set of *ab-initio* atomic charges. We have chosen the potential derived charges,³² which describe directly the electrostatic potential.

The effects of temperature and pressure are accounted for by computing the structures of minimum Gibbs energy $G(p, T)$ with a QHLD method.^{23,24,25} In this method, where the vibrational Gibbs energy of the phonons is estimated in the harmonic approximation, the Gibbs energy of the system is $G(p, T) = \Phi + pV + \sum_i h\nu_i/2 + k_B T \sum_i \ln[1 - \exp(-h\nu_i/k_B T)]$. Here V is the molar volume, $\sum_i h\nu_i/2$ is the zero-point energy, and the last term is the entropic contribution. The sums are extended to all phonon frequencies ν_i . Like pentacene, also tetracene exhibits *ab-initio* vibrational frequencies in the energy range of the lattice modes, and the coupling between lattice and intramolecular vibrations cannot be neglected.^{30,38} To account for it, we adopt an exciton-like model,^{31,36} where the interaction between different molecular coordinates is mediated by the intermolecular potential which depends directly on the atomic displacements. Since these correspond to the cartesian eigenvectors of the normal modes of the isolated molecule, we use the *ab-initio* eigenvectors and the scaled *ab-initio* frequencies. Intramolecular modes above 300 cm^{-1} are not taken into account, as the coupling is expected to be important only for low frequency modes.²⁹

IV. TEMPERATURE DEPENDENCE OF RAMAN SPECTRA AT CONSTANT PRESSURE

For tetracene two distinct bulk crystal structures have been detected by x-ray diffraction experiments. At room p, T conditions tetracene crystal was found to be triclinic,¹² space group $P\bar{1}$ (C_i^1). The unit cell contains two independent molecules located on the (0,0,0) and $(\frac{1}{2}, \frac{1}{2}, 0)$ inversion sites. Thus, the factor group analysis for the lattice phonons at $k = 0$ predicts six Raman active modes of A_g symmetry and three IR active modes of A_u symmetry. More recently Holmes *et al.*¹³ reported full data for crystalline tetracene at 183 K. As seen in section III, and unlike what found for pentacene,^{6,7} the two experimental structures of refs. 12,13 belong to a single polymorph. Finally, in 1985 Sondermann *et al.*¹⁹ identified by x-ray diffraction a second triclinic polymorph, for which unit cell parameters at 140 K were given, but it was not possible to determine whether the space group was $P\bar{1}$ or $P1$.

Room T Raman spectra of crystalline tetracene were reported in the late seventies by Jankowiak *et al.*,¹⁸ who also reported Raman spectra as a function of T . Discontinuous changes in the temperature dependence of Ra-

man lattice modes and the appearance of new phonon lines at 182 and 144 K were interpreted with the occurrence of two phase transitions,¹⁸ although some doubts could be harbored about the evidence of the high temperature (182 K) one. Also, a number of spectroscopic methods were used to test the occurrence of low temperature polymorphs in tetracene,^{14,15,16,17,39} yielding a quite large range of transition temperatures and conditions. The shattering of the sample upon cooling and large hysteresis effects upon heating the low T structure have been observed as a consequence of the phase transition.^{18,19}

With the aim of rationalizing the situation, we started the experiments by measuring Raman spectra at room p , T in the wavenumber range 20–300 cm^{-1} for samples grown by sublimation in a variety of ways, as described in section II. Depending either on the method of preparation or history of the samples, two different phonon patterns can be observed even at ambient conditions. To clarify the issue, we report in Figure 1 (bottom trace) the Raman spectrum at 298 K of the thin tetracene platelets typically obtained by sublimation under vacuum. In the same Figure (top trace) we also show the spectrum at the same temperature of samples grown in an inert at-

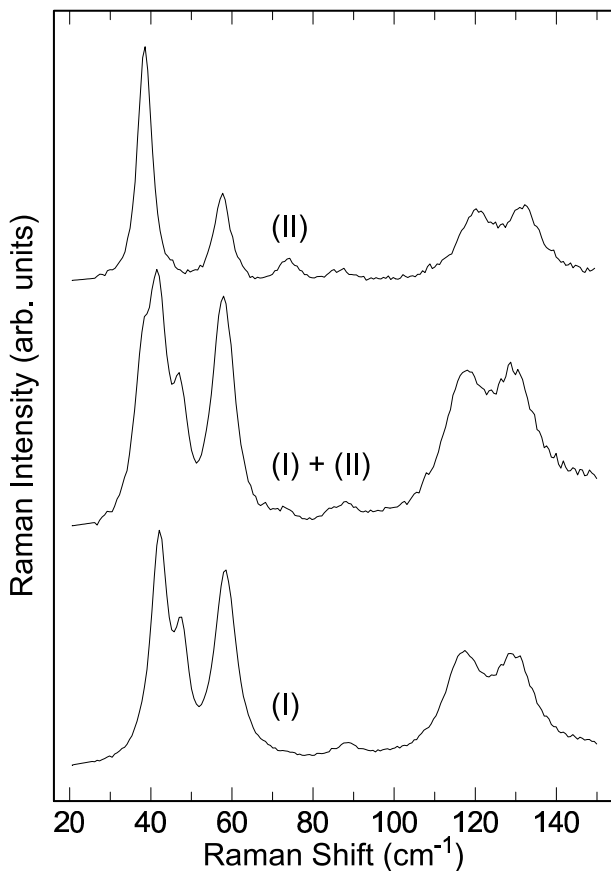


FIG. 1: Raman spectra at ambient p , T for tetracene polymorphs. Bottom: Polymorph I; Centre: Mixed phase; Top: polymorph II.

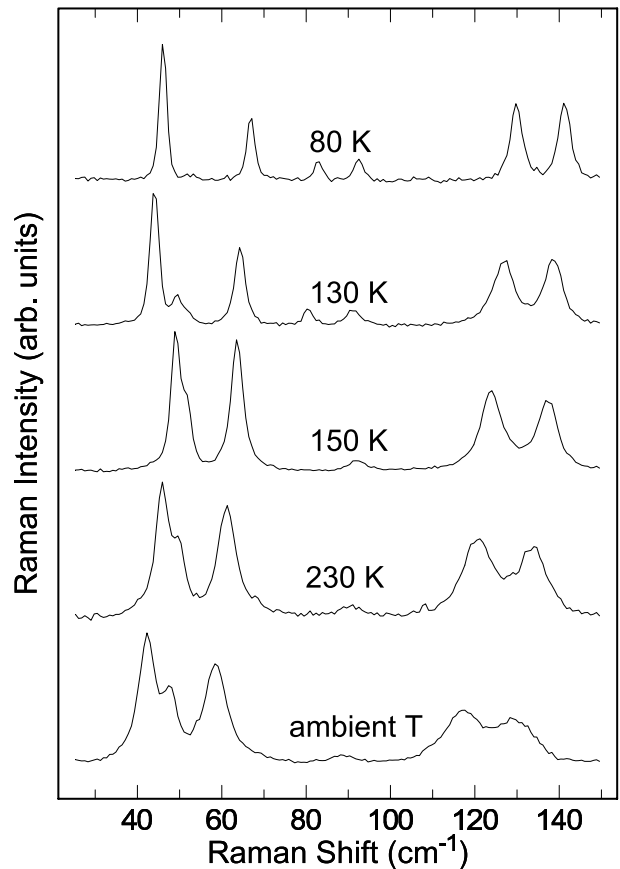


FIG. 2: Raman spectra of tetracene crystal as a function of T at ambient p .

mosphere at reduced pressure. Whereas the former spectrum agrees with that reported¹⁸ by Jankowiak *et al.* for the HT structure (hereafter called polymorph I), the latter is instead found to overlap the spectra of samples recovered at ambient conditions after both LT and HP cycles, as it will be shown in the following. Therefore, these samples correspond to another phase, which will be called polymorph II. Most microcrystalline specimens (Figure 1, centre trace) display the typical bands of polymorph I with additional features of variable intensity, which can be attributed to different amount of polymorph II present as physical impurity.

The phonon wavenumbers for polymorphs I and II at room T are given in Table I. Since the number of Raman bands observed for polymorph II is always six, as for polymorph I, it is likely that also polymorph II belongs to the $P\bar{1}$ space group symmetry. As already revealed by the spectra of Figure 1, the phonon pattern of the two polymorphs differs especially in the lowest frequency region. Polymorph I displays three closely grouped bands in the range 42–58 cm^{-1} , while polymorph II shows three evenly spaced bands in the range 38–73 cm^{-1} . We remark that this finding closely resembles what already reported for polymorphs **C** and **H** of pentacene,⁷ respectively.

For the low temperature measurements we chose the

TABLE I: Raman wavenumbers (cm^{-1}) of the lattice and intramolecular modes up to 240 cm^{-1} for polymorphs I and II of tetracene. We report the experimental A_g wavenumbers, the corresponding minimum $G(p, T)$ calculations, and, for the intramolecular modes, the *ab-initio* frequency and symmetry of the parent mode in the isolated D_{2h} molecule.

Polymorph I		Polymorph II				<i>ab-initio</i>		
298 K		80 K		298 K				
expt.	calc.	expt.	calc.	expt.	calc.	freq.	sym.	
42.3	36.5	46.1	31.4	38.3	24.4			
47.8	44.8	66.9	66.1	57.4	55.0			
58.5	62.0	83.2	75.6	73.0	65.4			
88.4	88.8	93.2	94.3	86.1	81.7			
117.1	131.3	129.9	151.7	118.8	136.1			
129.8	139.1	141.2	158.6	130.4	144.3			
168.2	175.2	166.7	172.0	165.1	164.6	}	146.5	b_{1g}
	176.4	172.9	184.8	171.2	175.3			
211.2	222.1	214.9	230.3	213.3	221.3	}	188.2	b_{2g}
217.0	225.3	218.6	231.7	217.8	223.0			

thin platelets of physically pure polymorph I, to assure that the starting material for the temperature cycling was physically homogeneous and belonging to the structure thermodynamically stable at ambient conditions. Selected spectra recorded on decreasing temperature in the range 298–80 K are shown in Figure 2. No discontinuities were seen in our samples down to 140 K. At 130 K the abrupt appearance of the pattern typical of polymorph II is observed in the low frequency phonon region. The spectral changes are either accompanied or preceded by a cracking of the crystal. However, unlike what reported by Jankowiak *et al.*,¹⁸ there is no hint of an intermediate crystal modification occurring in the range 180–140 K, even after repeated temperature cycling on several different specimens. The phase transformation is clearly completed at 80 K, where no features of the high temperature spectrum remain. The phonon wavenumbers of the 80 K spectrum of Figure 2 are reported in Table I, and should be compared with the (incomplete) spectrum at 77 K of ref. 18.

Interesting information can be obtained by repeated temperature cycling, as shown in Figure 3, where we display a sequence of spectra of a single sample. After the temperature transition has occurred (Figure 3 a,b), a large hysteresis is documented by the persistence of polymorph II upon heating up to 298 K, where all spectral features of this phase are still retained on the time scale of the experiment, as shown in Figure 3 c. Note that the latter spectrum overlaps the top one of Figure 1. This hysteresis effect allowed us to measure the temperature dependence of the phonon bands for polymorph II by cooling the sample over the same T range of polymorph I (Figure 3 d). Only by heating again polymorph II up to 320 K the conversion to polymorph I begins, although the process could be completed only by annealing at 400 K (Figure 3 e). The data will be compared with calculations in Section VI.

To summarize, two polymorphs have been clearly identified by the Raman analysis as function of temperature.

Polymorph I is the most frequently grown, and it is the form stable at room T . Polymorph II is the form ob-

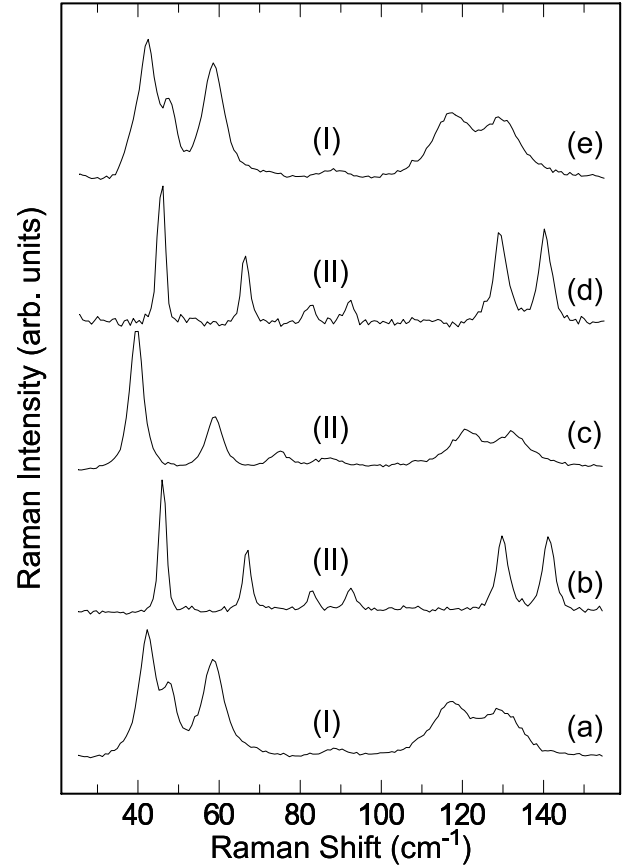


FIG. 3: Raman spectra of a single sample of pentacene subjected to repeated temperature cycling: (a) starting sample of polymorph I at 298 K; (b) the sample is transformed to polymorph II by cooling at 80 K; the features of polymorph II are retained both after (c) returning to ambient T and (d) cooling to 80 K; (e) polymorph I at 298 K is obtained again after annealing II at 400 K.

tained by lowering temperature below 140 K. However, it can be obtained as a (metastable) phase also at room T , either by sublimation at 493 K at reduced pressure in an inert atmosphere or by bringing back to room T samples cooled down to 80 K.

V. RAMAN SPECTRA UNDER PRESSURE

High pressure induced transformations in tetracene crystals were observed as discontinuous changes of the Davydov splitting in the electronic absorption spectrum,²⁰ spatial anisotropy of the magnetic field effect on fluorescence⁴⁰ and recently by studying the photoconductivity of tetracene single crystals.²¹ Mechanical stress induced by sample grinding was reported to produce a mixture of different phases.^{18,19} So far, no Raman spectra were reported for the pressure induced transformation, and no satisfactory characterization was performed for the HP phase. Starting from polymorph I, we have tried to record Raman spectra as a function of p over the range 0–6 GPa. However, in all samples and for all measuring conditions a strong fluorescence emission hides the Raman scattering above 1.4 GPa, and even in lower pres-

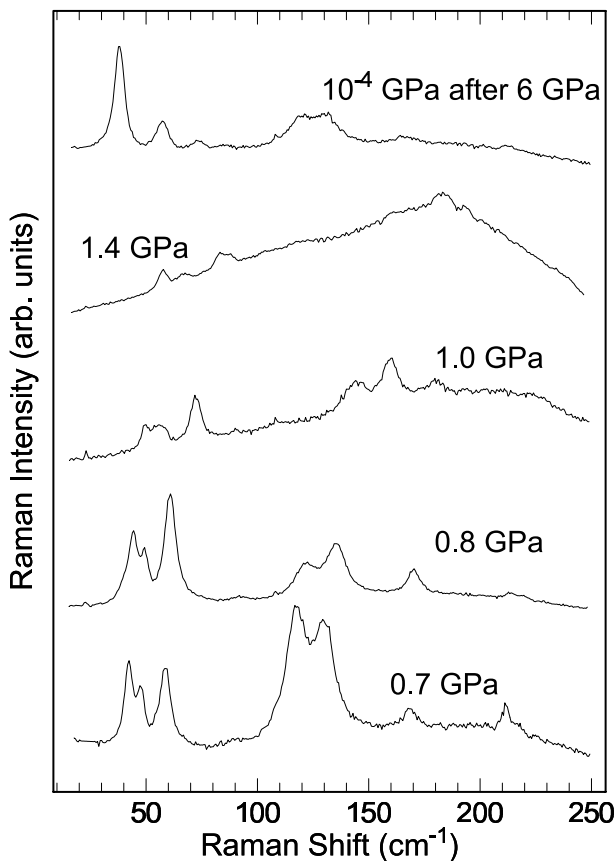


FIG. 4: Raman spectra of crystal tetracene as a function of p at ambient T , showing the transition from polymorph I to polymorph II in the sample recovered after compression.

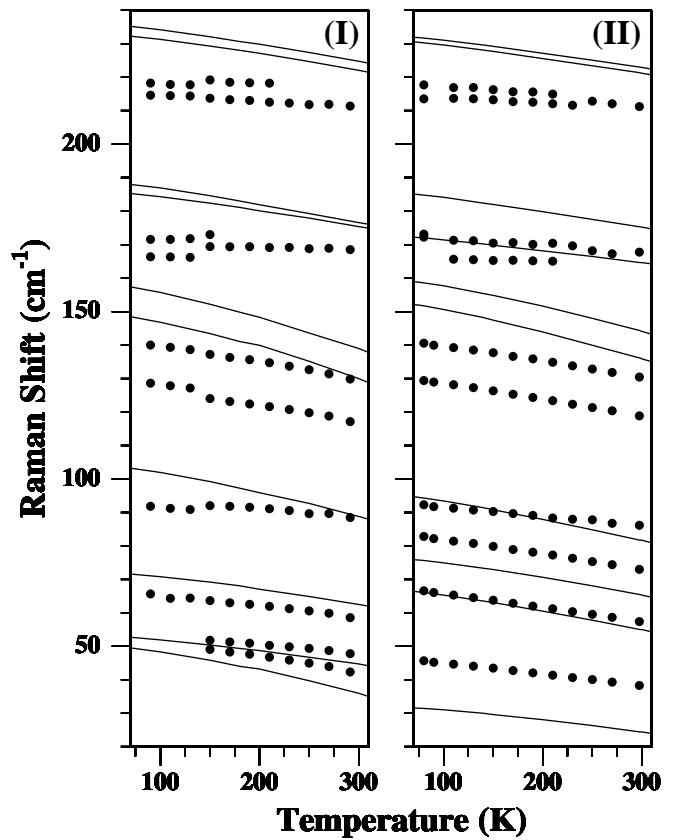


FIG. 5: Phonon wavenumbers *vs* temperature for polymorphs I (left) and II (right) of tetracene. Circles: Raman experiments. Lines: calculations for A_g phonons.

sure regimes the detection of all bands of the spectrum turns out to be quite difficult, as shown in Figure 4. Raman spectra of our samples show that even at 1.0 GPa there is no sign of phase change. Therefore, the onset of the pressure-induced phase transition is well above the value (around 0.3 GPa) previously reported^{20,21,40} with different experimental techniques. In any case, the investigation of the samples recovered at ambient p clearly shows that a complete transformation has taken place, as the spectrum displays all the bands polymorph II and none of polymorph I (Figure 4). Therefore, polymorph II can be obtained from polymorph I also by pressure cycling, in addition to temperature cycling described in the previous Section.

VI. COMPUTATIONAL RESULTS

We now describe the computational results, which help to definitely clarify the nature of the two tetracene polymorphs identified through Raman spectroscopy. In an early stage of our work, we considered separately the two complete experimental structures.^{12,13} Each structure was modeled starting from its experimental molecular arrangements, by replacing the experimental molecu-

TABLE II: Lattice parameters of tetracene. The experimental structures of refs. 12,13,19 are compared to the minimum Φ structures and to the minimum $G(T)$ structures calculated at the same temperature T (K) of the experiments. Energies are in kcal/mole, unit cell axes a , b , c are in Å, angles α , β , γ in degrees, and cell volumes V in Å³.

Structure	T	Energy	a	b	c	α	β	γ	V
Polymorph I									
Expt. ¹³	180		6.0565	7.8376	12.5523	101.275	99.453	94.208	572.968
Expt. ¹⁹	293		6.06	7.91	12.62	101.87	99.23	94.09	581.64
Expt. ¹²	298		6.03	7.90	12.70	101.68	98.65	93.70	582.85
Calc. min. Φ^a		-36.2612	5.8136	7.7098	12.5972	101.310	98.272	93.548	545.537
Calc. min. Φ^b		-36.2613	5.8133	7.7085	12.6008	101.335	98.266	93.542	545.538
Calc. min. G	180	-37.9681	5.8415	7.8507	12.6665	101.353	98.437	93.569	560.855
Calc. min. G	298	-42.4059	5.8745	7.9384	12.7224	101.281	98.471	93.568	572.940
Polymorph II									
Expt. ¹⁹	140		5.99	7.74	12.32	101.30	100.74	94.0	546.78
Calc. min. Φ^c		-35.9089	5.9411	7.5882	12.8064	106.123	97.980	85.594	548.818
Calc. min. G	140	-36.5954	5.9646	7.6820	12.8834	106.347	98.017	85.638	560.497

^aMinimum Φ structure for polymorph I computed starting from the structure of either ref. 12 or ref. 13.

^bDeepest potential energy minimum.²⁶

^cSecond deepest potential energy minimum.²⁶

lar geometries with the *ab-initio* one. We thus discovered that these two structures, measured at different T , actually map into the same potential minimum, having identical energies and unit cells (Table II). Therefore they correspond to a single phase, stable at room T , which we identify with polymorph I. Accordingly, the subsequent calculations for the T dependence of structure and dynamics for this polymorph were all performed starting from the data of Holmes *et al.*¹³ and *ab-initio* molecular geometry. In Table II, we compare the lattice parameters of the experimental structures of refs. 12,13,19 to the calculated parameters of the structures at the minimum of Φ and at the minima of $G(p, T)$. The latter were calculated at ambient pressure, and at the same temperatures of the experiments. As the various structures of the literature were not reported in the same standard crystallographic frame, we directly compare the equivalent reduced cells.⁴¹

In Table II we also report the minimum Φ lattice parameters of the structures which are theoretically predicted to correspond to the two deepest minima on the potential energy surface. These have been identified by performing a systematic search for the minima of the potential energy hypersurface. Following the methods used for pentacene⁸, we used a Quasi Monte Carlo sampling scheme to generate several thousands of different initial structures. Starting from each structure, we then minimized the total potential energy by adjusting the cell axes angles, positions and orientations of the molecules. The technical details of the calculations, together with information on the overall distribution of minima, will be reported in a separate paper.²⁶ Here we observe that the two deepest minima present triclinic lattice, space group $P\bar{1}$ (C_i^1), and differ mainly for the orientation of the two molecules in the unit cell. As shown in Table II, poly-

morph I of refs. 12,13,19 maps very accurately onto the deepest minimum of the potential energy surface. The table also shows that the minimum Φ structure for polymorph I reproduces reasonably well the experimental lattice parameters, with residual differences $\approx 3\%$ for the unit cell axes and angles. The computed cell volume is $\approx 5\%$ smaller than the experimental one at room temperatures. This discrepancy, which decreases upon cooling, is partly due to the thermal expansion, totally neglected in the minimum Φ calculations. In fact, as it can be seen from the results of the minimum $G(p, T)$ calculations, including vibrational effects brings the calculated volumes within 2% of the experimental ones, or better, and reproduces correctly the thermal expansion of phase I. The experimental volume expands by 1.7% from 180 to 298 K, to be compared with a calculated expansion of 2.1%. Finally, very good is the agreement for the experimental sublimation heat (unspecified phase) $\Delta_{\text{sub}}H = 34.4 \pm 1.2$ kcal/mol,⁴² which is to be compared with the Gibbs energy calculated at 0 K, $G(0) \approx 35.1$ kcal/mol.

A totally reliable comparison between our computed structures and the measurements for polymorph II is not currently feasible, since only the experimental cell parameters, and no atomic coordinates, are given in ref. 19. An accurate comparison is also impossible for the theoretical structures predicted in the same paper on lattice energy considerations. Note, however, that the prediction of a crystal symmetry lowering from $P\bar{1}$ to $P1$ is not supported by our Raman measurements.

In our calculations, we have found that the minimum $G(p, T)$ structure computed at 140 K starting from the second deepest minimum of the potential energy surface²⁶ favorably compares with the experimental cell parameters¹⁹ of polymorph II at the same T . The comparison is reported at the bottom of Table II, and al-

though the agreement with the experiment is with no doubt worse than for polymorph I, the association appears justified, and is well supported by the calculated phonon spectrum discussed below.

The experimental Raman frequencies recorded as a function of T for polymorphs I and II are compared to the corresponding minimum $G(p, T)$ calculations in Figure 5. The data for polymorph I are compared to the results obtained starting from the structure by Holmes¹³ *et al.*. Instead, the data for polymorph II are compared to those obtained by starting from the second theoretical deepest minimum.²⁶ Lattice and intramolecular modes are both shown. In Table I we report the calculated Raman wavenumbers for the two structures at 298 K, along with their experimental values. For polymorph II we also give the values at 80 K.

For both polymorphs the first six Raman modes are almost fully intermolecular in character, with negligible intramolecular contributions. In fact, the lowest *ab-initio* vibration of g symmetry in tetracene is calculated at 146.5 cm^{-1} , and is weakly coupled only with the highest frequency lattice mode, which displays a intramolecular contribution of about 10% at 80 K. Therefore, in the Raman spectra tetracene behaves as an apparent rigid-body while the coupling is expected to be important for ir active modes of u symmetry above 100 cm^{-1} , as already remarked by Filippini and Gramaccioli.³⁸

The temperature dependence of the phonon frequencies calculated for phases I and II (Figure 5), also agrees well with the corresponding experimental results. As expected, both experiments and calculations shows that varying the temperature affects the low frequency lattice modes much more than the purely intramolecular modes above 150 cm^{-1} . The differences between the experimental and computed temperature dependence of the frequencies, especially noticeable for the high frequency modes, are attributed to the anharmonic frequency shifts,⁴³ neglected in these calculations, and to defects in the potential model.

To summarize the results of the phonon dynamics analysis, we point out again (cf. section IV) that the patterns of the experimental frequencies for the lattice modes of polymorphs I and II at room T are clearly distinguishable, and are well matched by the patterns calculated for the experimental structure¹³ and for the second theoretical deepest minimum, respectively. In particular, the computations correctly predict the three closely spaced modes around 48 cm^{-1} for polymorph I, and reproduce the more widely spread bands between 38 and 73 cm^{-1} for polymorph II. Therefore we can associate polymorph I and II with the two deepest minima found in the potential energy surface.²⁶ Our calculations actually predict that polymorph I is the more stable (at 0 K) and denser phase, whereas experimentally the opposite is true. Moreover, we do not find theoretical evidence of the phase transition (crossing of G values) as function of either T or p . The same kind of problem has been found in calculations for pentacene.^{29,44} We could fine tune the atom-atom po-

tential to yield the correct phase ordering. On the other hand, the calculated energy difference between the two phases is very small, less than 0.5 kcal/mole , which is the typical accuracy of this kind of calculations. We therefore think that attempts to improve the potential would be unjustified at the present stage.

VII. DISCUSSION AND CONCLUSIONS

In this paper we have explored the p, T phase diagram of crystalline tetracene. By combining Raman spectroscopy with computational methods, we have clarified several issues related to the crystalline phases of tetracene. Tetracene crystallizes into two different polymorphs, polymorph I and II, the former being the most frequently grown phase, stable at ambient conditions. Whereas the crystalline structure of polymorph I is well known,^{12,13} we suggest a likely structure for polymorph II, stable at low T and high p . The structures of polymorph I and II are very similar to the structures of polymorph **C** and **H** of pentacene, respectively.²⁹ All structures are triclinic, space group $P\bar{1}$ (C_i^1), with two molecules per unit cell residing on symmetry unrelated inversion centers. In polymorph I and **C**, the long molecular axis is roughly pointing along the $[0,0,1]$ direction (c axis), in polymorphs II and **H**, which are the denser phases, the molecules are more inclined, and point towards the $[1,1,-1]$ direction. Raman spectroscopy in the lattice phonon region has indicated that the denser polymorph II of tetracene is stable only at low temperature (below 140 K) or high pressure (well above 1 GPa), whereas polymorph **H** of pentacene is the stable phase at ambient pressure. No additional phases have been detected, so early reports may have been affected by temperature induced strains and sample impurities/imperfections.²⁰

Finally, we have verified the possibility of obtaining either or both tetracene polymorphs at ambient p, T conditions, depending on sample preparation. Obtaining pure polymorph II at ambient conditions can be very important, as we expect that a denser phase should exhibit larger bandwidths and mobilities. The two tetracene phases are very similar in energy, and as it happens for pentacene, crystalline samples may show phase inhomogeneities. The two polymorphs can be easily identified through Raman spectroscopy in the lattice phonon region, and possible phase inhomogeneities are detectable this way. Raman spectroscopy thus represents a convenient and reliable tool for checking crystal quality, contributing to improve the performances of tetracene-based devices.

Acknowledgments

Work supported by the Consorzio Interuniversitario Nazionale per la Scienza e Tecnologia dei Materiali

(I.N.S.T.M., PRISMA2002 project) and by the Italian Ministero Istruzione, Università e Ricerca (M.I.U.R.,

FIRB project).

-
- ¹ D. J. Gundlach, J. A. Nichols, L. Zhou, and T. N. Jackson, Appl. Phys. Lett. **80**, 2925 (2002).
 - ² V. Y. Butko, X. Chi, and A. P. Ramirez, Solid State Commun. **128**, 431 (2003).
 - ³ R. W. I. de Boer, T. M. Klapwijk, and A. F. Morpurgo, Appl. Phys. Lett. **83**, 4345 (2003), and references therein.
 - ⁴ R. A. Laudise, Ch. Kloch, P. G. Simpkins, and T. Siegrist, J. Crystal Growth **187**, 449 (1998).
 - ⁵ M. Voigt, S. Dorsfeld, A. Volz, and M. Sokolowski, Phys. Rev. Lett. **91**, 026103 (2003).
 - ⁶ E. Venuti, R. G. Della Valle, A. Brillante, M. Masino, and A. Girlando, J. Am. Chem. Soc. **124**, 2128 (2002).
 - ⁷ A. Brillante, R. G. Della Valle, L. Farina, A. Girlando, M. Masino, and E. Venuti, Chem. Phys. Lett. **357**, 32 (2002).
 - ⁸ R. G. Della Valle, E. Venuti, A. Brillante, and A. Girlando, J. Chem. Phys. **118**, 807 (2003).
 - ⁹ C. C. Mattheus, A. B. Dros, J. Baas, G. T. Oostergetel, A. Meetsma, J. L. de Boer, and T. T. M. Palstra, Synth. Met. **138**, 475 (2003).
 - ¹⁰ T. Siegrist, Ch. Kloc, J. H. Schön, B. Batlogg, R. C. Haddon, S. Berg, and G. A. Thomas, Angew. Chem. Int. Ed. Engl. **40**, 1732 (2001).
 - ¹¹ C. C. Mattheus, A. B. Dros, J. Baas, A. Meetsma, J. L. de Boer, and T. T. M. Palstra, Acta Cryst. C **57**, 939 (2001).
 - ¹² R. B. Campbell, J. M. Roberston, and J. Trotter, Acta Crystallogr. **15**, 289 (1962).
 - ¹³ D. Holmes, S. Kumaraswamy, A. J. Matzger, and K. P. Vollhardt, Chem. Eur. J. **5**, 3399 (1999).
 - ¹⁴ A. F. Prikhotko and A. F. Skorobogatko, Opt. Spectrosc. **20**, 33 (1966).
 - ¹⁵ G. Vaubel and H. Bässler, Mol. Cryst. Liq. Cryst. **12**, 39 (1970).
 - ¹⁶ J. M. Turllet and M. R. Philpott, J. Chem. Phys. **62**, 4260 (1973).
 - ¹⁷ D. D. Kolendritskii, M. V. Kurik, and Yu. P. Piryatinskii, Phys. Status Solidi b **91**, 741 (1979).
 - ¹⁸ R. Jankowiak, J. Kalinowski, M. Konys, and J. Buchert, Chem. Phys. Lett. **65**, 549 (1979).
 - ¹⁹ U. Sondermann, A. Kutoglu, and H. Bässler, J. Phys. Chem **89**, 1735 (1985).
 - ²⁰ J. Kalinowski and R. Jankowiak, Chem. Phys. Lett. **53**, 56 (1978).
 - ²¹ Z. Rang, A. Haraldsson, D. M. Kim, P. P. Ruden, M. I. Nathan, R. J. Chesterfield, and C. D. Frisbie, Appl. Phys. Letters **79**, 2731 (2001).
 - ²² R. W. I. de Boer, M. Jochemsen, T. M. Klapwijk, A. F. Morpurgo, J. Niemax, A. K. Tripathi, and J. Pflaum, Appl. Phys. Lett., **95**, 1196 (2004).
 - ²³ W. Ludwig, *Recent Developments in Lattice Theory*, Springer Tracts in Modern Physics, Vol. 43 (Springer-Verlag, Berlin, 1967).
 - ²⁴ R. G. Della Valle, E. Venuti, and A. Brillante, Chem. Phys. **202**, 231 (1996).
 - ²⁵ R. G. Della Valle and E. Venuti, Phys. Rev. B **58**, 206 (1998), and references therein.
 - ²⁶ R. G. Della Valle, E. Venuti, A. Brillante, and A. Girlando, (in preparation, 2004), <http://www.chim.unifi.it/~valle/pub.html>.
 - ²⁷ LOTO Scientific Instruments; <http://www.loto-eng.com/>.
 - ²⁸ G. J. Piermarini, S. Block, J. P. Barnett, and R. A. Forman, J. Appl. Phys. **46**, 2774 (1975).
 - ²⁹ M. Masino, A. Girlando, R. G. Della Valle, E. Venuti, L. Farina, and A. Brillante, Mat. Res. Soc. Symp. Proc. **725**, 149 (2002).
 - ³⁰ R. G. Della Valle, E. Venuti, L. Farina, and A. Brillante, Chem. Phys. **273**, 197 (2001).
 - ³¹ A. Girlando, M. Masino, G. Visentini, R. G. Della Valle, A. Brillante, and E. Venuti, Phys. Rev. B **62**, 14476 (2000).
 - ³² M. J. Frisch, *et al.*; *Gaussian 98, Revision A.5* (Gaussian, Inc., Pittsburgh PA, 1998).
 - ³³ C. Lee, W. Yang, and R. G. Parr, Phys. Rev. B **37**, 785 (1988).
 - ³⁴ G. Rauhut and P. Pulay, J. Phys. Chem. **99**, 3093 (1995).
 - ³⁵ A. P. Scott and L. Radom, J. Phys. Chem. **100**, 16502 (1996).
 - ³⁶ S. Califano, V. Schettino, and N. Neto, *Lattice Dynamics of Molecular Crystals* (Springer-Verlag, Berlin, 1981).
 - ³⁷ D. E. Williams, J. Chem. Phys. **47**, 4680 (1967).
 - ³⁸ G. Filippini and C. M. Gramaccioli, Chem. Phys. Lett. **104**, 50 (1984).
 - ³⁹ J. Kalinowski, R. Jankowiak, and H. Bässler, J. Lumin. **22**, 397 (1981).
 - ⁴⁰ J. Kalinowski, J. Godlewski, and R. Jankowiak, Chem. Phys. Lett. **43**, 127 (1976).
 - ⁴¹ A. Santoro and A. D. Mighell, Acta Cryst. A **26**, 124 (1970).
 - ⁴² C. G. DeKruif, J. Chem. Thermodyn. **12**, 243 (1980).
 - ⁴³ R. G. Della Valle, P. F. Fracassi, R. Righini and S. Califano, Chem. Phys. **74**, 179 (1983).
 - ⁴⁴ S. Verlaak, S. Steudel, P. Heremans, D. Janssen and M. S. Deleuze, Phys. Rev. B **68**, 195409 (2003).